Microsyst Technol (2016) 22:275–282
DOI 10.1007/s00542-014-2388-0

TECHNICAL PAPER

Three-axis pneumatic tactile display with integrated capacitive sensors for feedback control

Seokpyo Yun · Jihyung Yoo · Soochul Lim · Joonah Park · Hyung-Kew Lee · Kwang-Seok Yun

Received: 3 November 2014 / Accepted: 26 November 2014 / Published online: 10 December 2014

Abstract In this paper, we propose a three-axis pneumatic tactile display that is precisely controlled by using integrated capacitive displacement sensors. The proposed tactile display consists of a core body with a 3 × 3 balloon array on its top surface, four lateral balloons made of latex rubber, and inner and outer frames that include capacitive displacement sensors based on a flexible printed circuit board. The 3 × 3 balloon array on the core body is designed to apply normal haptic stimulation to a human fingertip. In addition, the lateral motions of the core body and each frame produce haptic stimulation in a tangential direction. Precise control of lateral motion was achieved by feedback control using the capacitive displacement sensors. The size of the fabricated tactile display was 26 × 26 × 18 mm^3. We experimentally performed manipulation of the proposed device with a custom control system, thereby demonstrating accurate control of displacement.

S. Yun and J. Yoo contributed equally to this work.

S. Yun · J. Yoo · K.-S. Yun (✉)
Department of Electronic Engineering, Sogang University, 35 Baekbeom-ro, Mapo-gu, Seoul 121-742, Korea
e-mail: ksyun@sogang.ac.kr

S. Lim · J. Park
Samsung Advanced Institute of Technology, San 14, Nongseo-dong, Giheung-gu, Yongin-si, Gyunggi-do 446-712, Korea

H.-K. Lee
Center for Electricity and Magnetism, Korea Research Institute of Standards and Science, 267 Gajeongro, Yuseong-gu, Daejeon 305-340, Korea

1 Introduction

Drastic development of medical devices has contributed to the advancement of modern medical sciences. In addition, modern electrical and mechanical engineering has been widely utilized in various medical devices, increasing their performance. The robotic surgical system is among the most advanced medical equipment using integration of the various engineering technologies (Lanfranco et al. 2004; Corcione et al. 2005; Muller-Stich et al. 2007; Schreuder and Verheijen 2009).

The most widely used robotic surgical system is the daVinci surgical system, which was first introduced to market in 1999 by Intuitive Surgical, Inc. The system performs effective laparoscopy with bending motion, rotating motion, and three-dimensional (3D) endoscopic viewing inside the human body. The surgeon performs the surgery by controlling surgical devices such as forceps, needles, and retractors that are attached to the robot arms. During the surgery, the surgeon stays in a separate space from the patient, watching the real-time image through the endoscope.

The advantages of robotic surgery include precise control beyond the abilities of human hands, minimized incision, and quick recovery due to minimally invasive techniques. Despite these merits, the physical isolation between the surgeon and the patient is an issue to be resolved for stable surgical operation. Physical isolation makes a surgeon insensitive to the force that surgery robots apply to a patient because only visual information is available. This implies that a surgery may have different results from the surgeon's use of experience and skill. If the surgeon applies excessive force during surgery, unnecessary bleeding or improper damage can occur (Sung and Gill 2001; Ballantyne 2002; Hashizume et al. 2002; Kornprat et al. 2006; Morino et al. 2006).

A device displaying tactile information reportedly solves this problem because haptic stimuli have been found to be more effective than visual data (Dargahi and Najarian 2003; Dargahi et al. 2007; Reiley et al. 2008) in providing tactile information (Bethea et al. 2004; Lamata et al. 2006). Several haptic devices that stimulate the tactile sense have been reported (Kim et al. 2004; Ottermo et al. 2008; Moradi Dalvand et al. 2014b), showing that realistic haptic feedback helps an operator perform with better skills (Tholey et al. 2005; Wottawa et al. 2013; Moradi Dalvand et al. 2014a).

King et al. reported tactile displays for robot-assisted surgery (Culjat et al. 2008; King et al. 2008). The device was composed of a pneumatic tactile display that included six inflating balloons controlled using feedback signals from force sensors that measured the grasping force applied to an organ. They demonstrated that performance could be improved by using the proposed system in an in vivo test with surgeons dissecting animal subjects. One drawback of the haptic display developed by King et al. is that the device can only deliver normal force. It is known that both normal and tangential forces to the human finger are also important for humans to feel real haptic stimulation (Bark et al. 2013).

In our previous work, we reported a tactile display that could express both normal and tangential forces by using pneumatic pressure (Doh et al. 2013; Lim et al. 2014). The tangential display was obtained by actuation of a solid structure tangential to a finger surface. Because a pneumatic pressure regulator passively controlled the tangential actuation, the device suffered from hysteresis resulting in poor position accuracy. In order to solve this problem, we demonstrated a tactile display that was controlled by a position feedback signal. Though this device showed that it was possible to solve the hysteresis problem, it suffered from unstable position sensing because the position sensor was affected by normal pressure from the fingertip (Yoo et al. 2014). Therefore, in this paper we propose a three-axis tactile display with integrated capacitive position sensors that are formed on sidewalls of moving components to obtain accurate tangential movement; they have active feedback control, and circumvent the influence of normal pressure.

2 Design

Figure 1 shows a schematic view and an exploded diagram of the proposed three-axis tactile display. The device is composed of a core body, inner frame, and outer frame. The core body in the middle has nine circular balloons on its top surface, and a pair of elliptical balloons on its side surfaces. Each balloon is made of a 600 µm thick latex membrane covering the holes or pressure chambers, which are

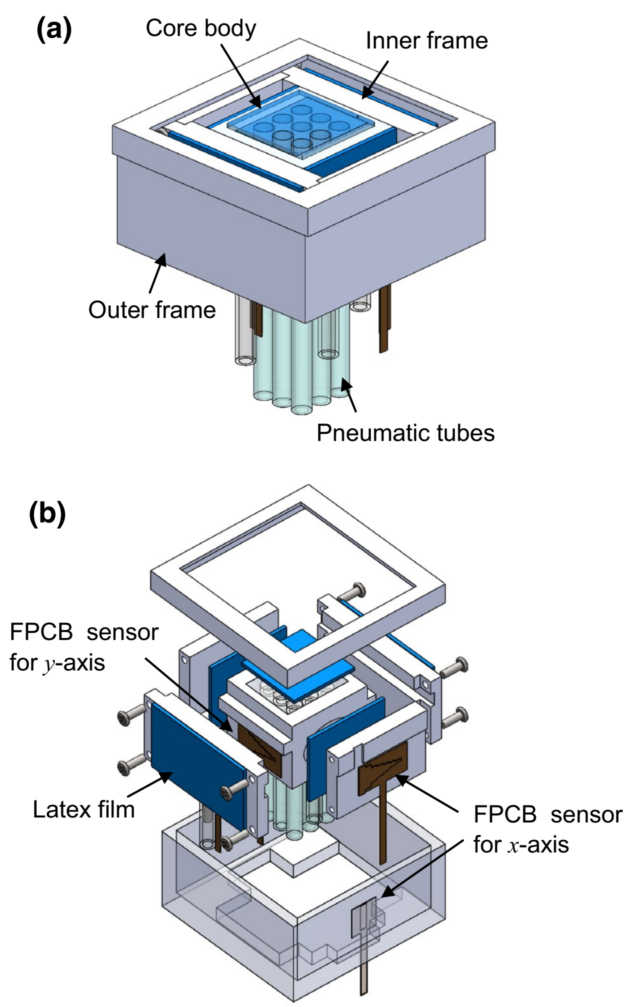

Fig. 1 Overall structure of the proposed 3-axis haptic device. **a** Assembled and **b** exploded view

connected to silicone tubes for the application of pneumatic pressure. When air pressure is applied to the silicone tubes, the circular balloons on the top surface inflate, and a fingertip placed on top of the device feels normal haptic stimulation. As shown in Fig. 1b, the core body is guided by the inner frame, and moves only in the y-axis direction. Groove structures are formed on the inner surface of the inner frame to guide the rail structure of the core body. A pair of flexible printed circuit board (FPCB) sheets with patterned electrodes is attached to each wall of the core body and inner frame to form a capacitive sensor that measures the position of the core body in the y-direction. The lateral movement of the core body in the y-direction is actuated by the inflation of the balloons on the core body's sidewall as shown in Fig. 2. Similarly, the inflation of balloons on the inner frame's sidewall actuates the inner frame in the x-direction, which is monitored by the capacitive position sensor formed on each wall of the inner and outer frames.

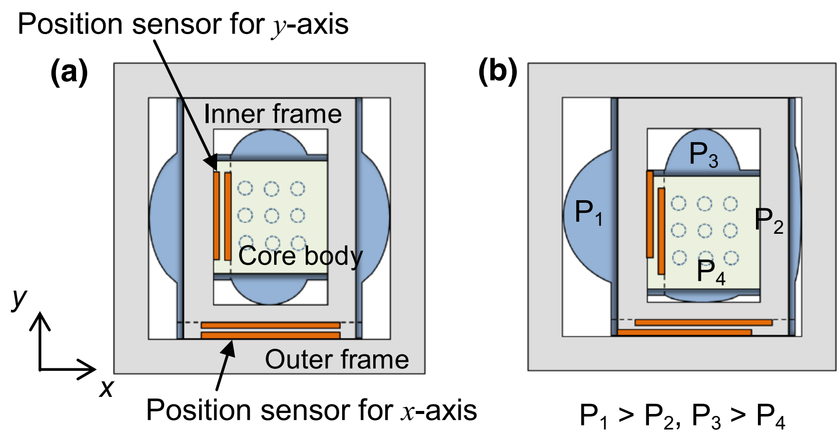

Fig. 2 **a** Top view of device, **b** tangential actuation by pneumatic pressure difference applied on each side balloon

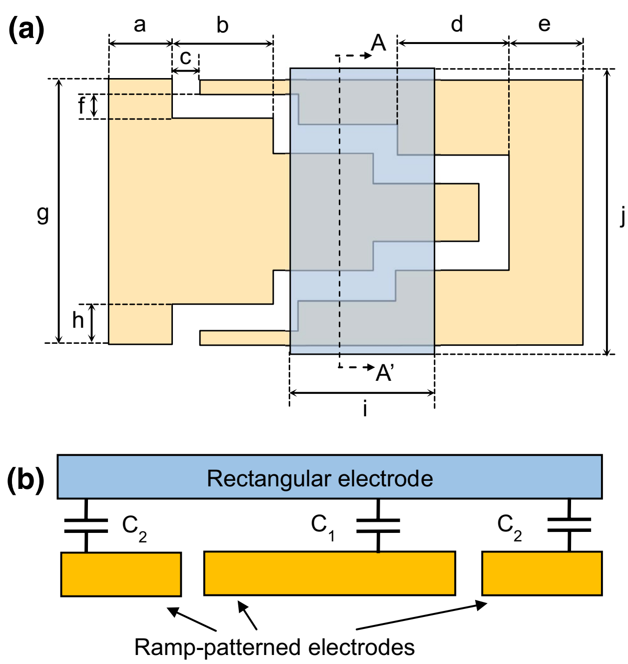

Fig. 3 Schematic of the capacitive displacement sensor: **a** layout of rectangular shape and ramp-patterned electrodes, **b** its cross-sectional view at the A–A' line

Table 1 Dimensions for capacitive position sensor

Parameters	Dimension (mm)
a	1.0
b	1.0
c	0.1
d	1.0
e	1.0
f	0.1
g	3.5
h	0.2
i	2.0
j	4.5

The outer frame is designed to enclose the inner frame, and restricts its movement in the y-direction. Tangential movement of the device is performed by two pairs of balloons at the sidewalls of the core body and the inner frame as shown in Fig. 2. When external pneumatic pressure is applied to the device, air inflates the balloons, which pushes the structure laterally. The lateral x–y position of the core body is determined by the difference in pressure on the balloons in opposition to each other.

Figure 3 shows the schematic of the capacitive displacement sensor integrated into the tactile device. The sensor is composed of two FPCB layers: one has a rectangular electrode; and the other has two ramp-patterned electrodes. Two parallel-plate capacitors, C_1 and C_2, are formed between a rectangular electrode and each of ramp-patterned electrodes. The capacitance of each capacitor varies when the ramp-patterned electrodes move in a lateral direction as the core body or inner frame do by lateral actuation. The ramp-patterned electrodes have been used to obtain a linear output value according to the electrode's position (Baxter 1997). To improve the sensitivity of the sensor, the slope of the ramp pattern should be increased. Further, the initial capacitance must be large enough to minimize the influence of the parasitic capacitance. Considering these design parameters and the restricted area for the sensor unit, we determined the dimensions of electrodes as shown in Table 1.

3 Implementation

3.1 Device

Figure 4a shows a photograph of a fabricated three-axis pneumatic tactile display. Each part of the device was made of polycarbonate by using machining whose

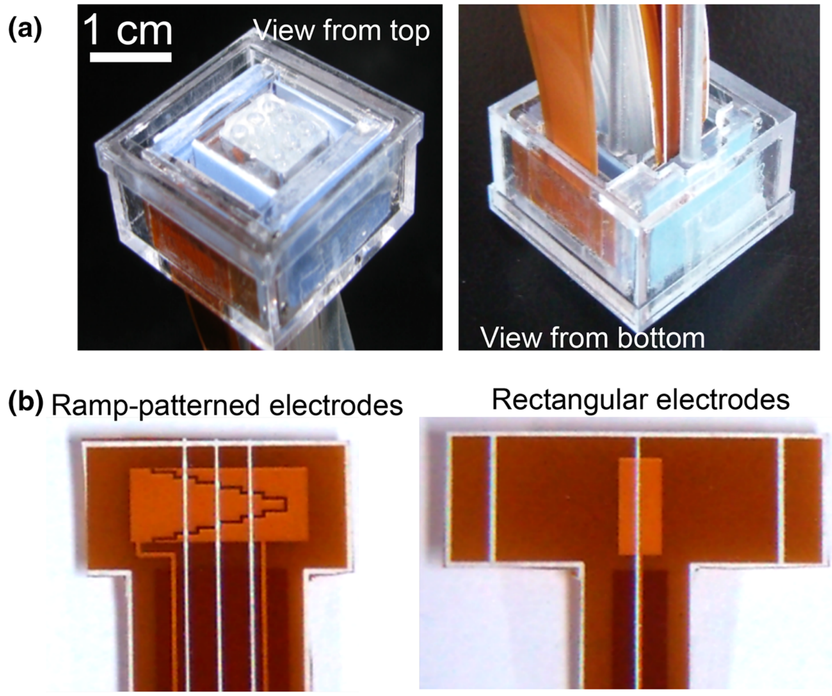

Fig. 4 **a** Photograph of the fabricated three-axis pneumatic tactile display, **b** photo of fabricated capacitive position sensor

tolerance was less than 100 µm. The sidewall balloons were made of 600 µm thick latex film that was attached to each side of processed polycarbonate structures. The top surface of the core body was attached with 100 µm thick latex film to form nine balloons generating normal tactile actuation. Silicone tubes were connected to the bottom of the structure to apply pneumatic pressure. All of the structures, including the core body, inner frame, outer frame, and cover were manually assembled to complete the device fabrication. Figure 4b is a photo of the fabricated capacitive position sensor. The sensors were manufactured with FPCB using copper electrodes. The signal lines were positioned over a shielding metal layer to block high-frequency environmental noise. As described in Sect. 2 and shown in Figs. 2 and 4, the sensors for measuring the x- and y-positions were formed in the gaps between the inner and outer frame, and inner frame and core body, respectively. After the complete assembly of the tactile display, the minimum and maximum capacitances were measured as 0.12 and 1.56 pF, respectively.

3.2 Feedback control unit

Figure 5a shows a block diagram of the overall feedback-controlled tactile display system. A total of four capacitance values from two capacitive sensors were read and converted into corresponding voltage values successively by a readout circuit. Then data was transferred to a computer through a data acquisition device (DAQ, NI USB-6259, National Instruments) to calculate the current position of the actuation body using LabVIEW (National Instruments) software. A feedback-control algorithm controlled the actuator body by generating control signals for the pneumatic pressure regulators after comparing the current and target positions.

The readout circuit for measuring capacitance values was based on the switched-capacitor method, as shown in Fig. 5b. In this circuit, an amplifier circuit through a switch block sequentially read each of four capacitors. The output voltage signal was stabilized with a regulator and an R–C filter circuit. A complex programmable logic device (CPLD, XC2C64A_7VQG44C, Xilinx) controlled the timing of the switching. Figure 5c is a photo of the readout circuit board, including power unit, clock generator, CPLD, and capacitance readout unit. It took 12 µs to read a single capacitance value, which resulted in an operational frequency of 20.8 kHz.

4 Results and discussion

The inflation of a balloon for normal tactile actuation on the core body was monitored using a camera while applying pneumatic pressure. As shown in Fig. 6, the center deflection was linearly proportional to the applied pressure (King et al. 2008) and was measured at about 1.5 mm under a pressure of 110 kPa.

The capacitive sensor was verified by measuring the voltage output signals from readout circuit. The output

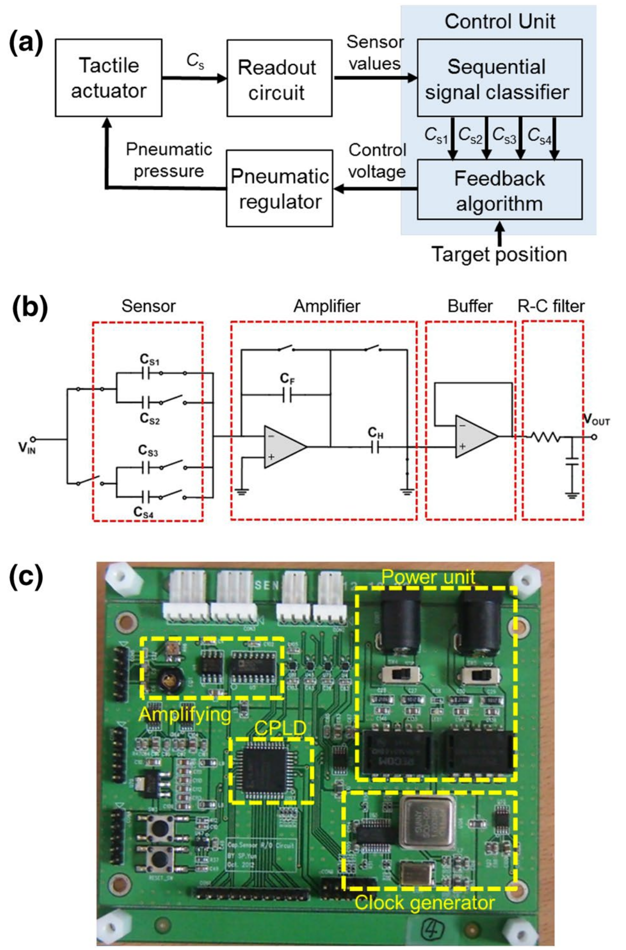

Fig. 5 **a** Overall block diagram of the implemented tactile feedback system, **b** schematic of the capacitive readout circuit, **c** a readout circuit board

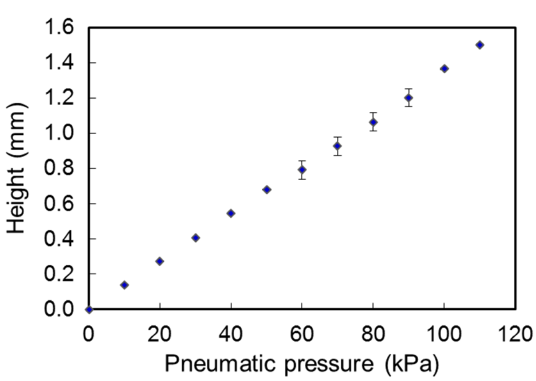

Fig. 6 Center deflection of balloons on top surface of the core body for various pneumatic pressures

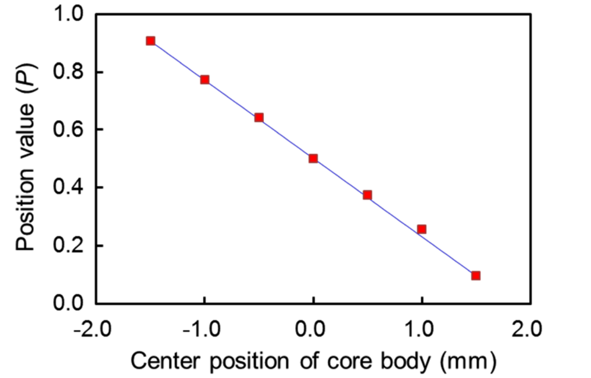

Fig. 7 Position value (P) output from capacitive sensor through readout circuit for various lateral position of the core body

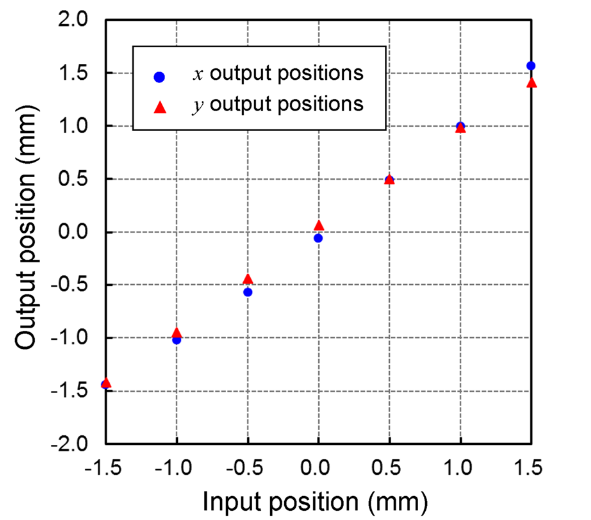

Fig. 8 Center position of core body in x- and y-direction for various input target positions

signals, V_{out1} and V_{out2}, from each capacitor formed by a common rectangular electrode and two ramp-patterned electrodes, can be expressed as

$$V_{out1} = V_{in} \frac{C_{s1}}{C_F} \tag{1}$$

$$V_{out2} = V_{in} \frac{C_{s2}}{C_F} \tag{2}$$

where V_{in} is input voltage, and C_F is feedback capacitance in Fig. 5, which in our design were 5 V and 2 pF, respectively. The position value (P) of the core body can be expressed using V_{out1} and V_{out2} as follows:

$$P = \frac{V_{out1}}{V_{out2} + V_{out2}} = \frac{C_{s1}}{C_{s1} + C_{s2}}. \tag{3}$$

The device was designed to have a position value ranging from 0.07 to 0.93, while the actuator body moves ±1.5 mm in the lateral direction. The position value becomes 0.5 when the actuator body is at the center, locating the rectangular electrode at the center of ramp-patterned electrodes. In this work, the output value was measured at seven points with 0.5 mm of lateral movement. As shown in Fig. 7, the position values from the capacitive position sensor varied linearly with the lateral position of core body, showing very good agreement with the theoretical value. The largest discrepancy for the target position was measured as 0.04 mm for a moving distance of 1 mm, which might be caused by parasitic capacitance formed by wiring metal lines in the FPCB capacitive sensor units. We have compensated for this embedded error in the feedback control algorithm to achieve accurate position control.

The positioning accuracy is shown in Fig. 8. We moved the actuation body to seven different positions in both of x- and y-directions. Blue dots in this graph show the positions of the inner frame moving along the x-axis, while the position on the y-axis is fixed at the center. The data was averaged after measuring the position three times. Our previous tactile display system, without feedback control, showed severe hysteresis, resulting in poor repeatability and inaccurate positioning (Doh et al. 2013). Using capacitive feedback control in this work, the proposed tactile display showed very linear operation and good repeatability in position, with very low hysteresis. The y-directional position control is shown with red dots where the position of the core body moving along the y-axis was measured while maintaining the x-position at the center. The average discrepancy was 0.04 and 0.06 mm for *x*- and *y*-directional movement, respectively. The larger discrepancy in *y*-directional movement might be related to the size of the actuation balloons. The balloons actuating the body in the y-direction were relatively small because of the restricted sidewall area of the core body. As the dimension of balloon decreased, more pneumatic pressure was required, which resulted in large operation error.

Two-dimensional control accuracy was monitored by repeatedly measuring the difference between the target position and the actual destination. It was measured three times, for a total of nine points at intervals of 0.5 mm in each axis, as shown in Fig. 9a. In that figure, the measured moving positions are marked as dots with different colors and shapes for three repeated tests. The control accuracy was measured as 0.11 mm in both x- and y-directions. Because a human finger can discriminate a spatial tangential resolution of more than 2 mm, the accuracy of our device will be enough for application in tactile display.

Figure 9b shows photographs of tangential actuation at nine different positions: (−1.5, 1.5), (0, 1.5), (1.5, 1.5), (−1.5, 0), (0, 0), (1.5, 0), (−1.5, −1.5), (0, −1.5), and (1.5, −1.5). Here, the top surface of the core body was covered with a thin paper that had marks measuring the displacement.

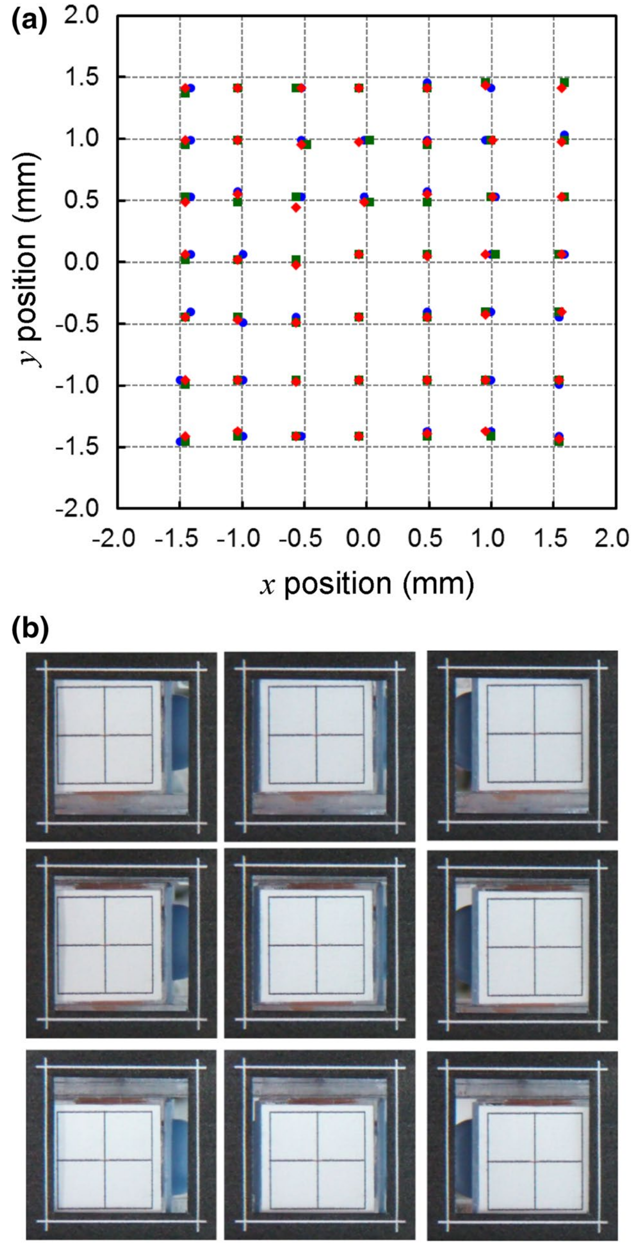

Fig. 9 **a** 2-D plot of output positions from three repeated tests with input target positions (*crossing points of dashed lines*), **b** photographs of the actuator at nine different output positions

Finally, we considered the lateral positioning accuracy when normal pressure is applied to the actuator, because the grasping motion of a finger will push the core body in the normal direction. To evaluate this, we measured the tangential motion of the core body in the y-direction while applying normal force to the core body. The core body was moved to five different target positions while varying the force from 0 to 4 N. As shown in Fig. 10, the positioning was quite accurate regardless of the normal force, which is an important advantage of our feedback control-based actuator.

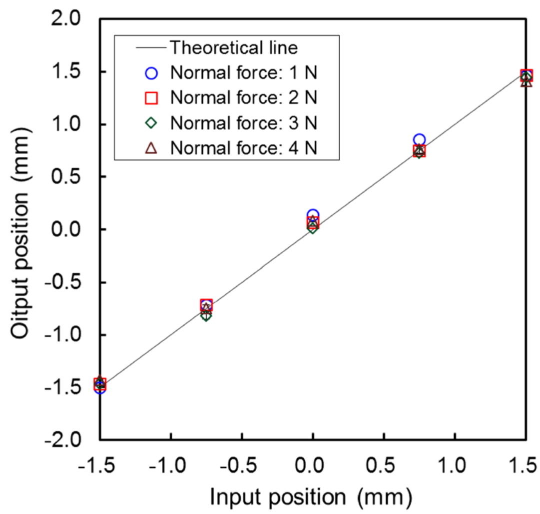

Fig. 10 Accuracy of output positions under various normal forces on the core body

5 Conclusions

In this paper, we developed and demonstrated a three-axis pneumatic tactile display integrated with capacitive displacement sensors for feedback position control. By integrating capacitive sensors for feedback control onto the sidewalls of moving structures, we could obtain accurate control of tangential displacement regardless of the normal force applied to the device. The structure was made of polycarbonate with the use of precise machining. We achieved tangential 2-D actuation by applying pneumatic pressure on sidewall balloons, and consequently moving the core body in lateral directions. In addition, nine balloons were formed on the top surface of the core body to generate normal tactile stimulation on a fingertip. The pressure on each balloon was controlled accurately using electro-pneumatic regulators and LabVIEW. The size of the tactile display was $26 \times 26 \times 18$ mm^3 and the accuracy of lateral position control was measured at 0.11 mm. In this study, we demonstrated that the accuracy of a three-axis tactile display can be improved by integrating a feedback control unit, and will be a good candidate as a tactile feedback application for robot-assisted surgical systems.

Acknowledgments This work was supported by Samsung Advanced Institute of Technology.

References

Ballantyne G (2002) Robotic surgery, telerobotic surgery, telepresence, and telementoring: review of early clinical results. Surg Endosc 16(10):1389–1402

Bark K, Mcmahan W, Remington A, Gewirtz J, Wedmid A, Lee DI, Kuchenbecker KJ (2013) In vivo validation of a system for haptic feedback of tool vibrations in robotic surgery. Surg Endosc 27(2):656–664

Baxter LK (1997) Capacitive sensors. IEEE Press, New York

Bethea B, Okamura A, Kitagawa M, Fitton T, Cattaneo S, Gott V, Baumgartner W, Yuh D (2004) Application of haptic feedback to robotic surgery. J Laparoendosc Adv Surg Tech 14(3):191–195

Corcione F, Esposito C, Cuccurullo D, Settembre A, Miranda N, Amato F, Pirozzi F, Caiazzo P (2005) Advantages and limits of robot-assisted laparoscopic surgery: preliminary experience. Surg Endosc 19(1):117–119

Culjat M, King C, Franco M, Bisley J, Grundfest W, Dutson E (2008) Pneumatic balloon actuators for tactile feedback in robotic surgery. Ind Robot Int J 35(5):449–455

Dargahi J, Najarian S (2003) An endoscopic force-position sensor grasper with minimum sensors. Can J Electr Comput Eng 28(3/4):155–161

Dargahi J, Najarian S, Ramezanifard R (2007) Graphical display of tactile sensing data with application in minimally invasive surgery. Can J Electr Comput Eng 32(3):151–155

Doh E, Yoo J, Lee H, Park J, Yun K (2013) Microfabrication of three-axis tactile feedback actuator for robot-assisted surgery. Jpn J Appl Phys 52:017302

Hashizume M, Shimada M, Tomikawa M, Ikeda Y, Takahashi I, Abe R, Koga F, Gotoh N, Konishi K, Maehara S, Sugimachi K (2002) Early experiences of endoscopic procedures in general surgery assisted by a computer-enhanced surgical system. Surg Endosc 16(8):1187–1191

Kim D, Kim B, Kang H (2004) Development of a piezoelectric polymer-based sensorized microgripper for microassembly and micromanipulation. Microsyst Technol 10(4):275–280

King C, Franco M, Culjat M, Higa A, Bisley J, Dutson E, Grundfest W (2008) Fabrication and characterization of a balloon actuator array for haptic feedback in robotic surgery. J Med Devices 2(4):041006

Kornprat P, Werkgartner G, Cerwenka H, Bacher H, El-Shabrawi A, Rehak P, Mischinger HJ (2006) Prospective study comparing standard and robotically assisted laparoscopic cholecystectomy. Langenbecks Arch Surg 391(3):216–221

Lamata P, Gómez E, Sánchez-Margallo F, Lamata F, Del Pozo F, Usón J (2006) Tissue consistency perception in laparoscopy to define the level of fidelity in virtual reality simulation. Surg Endosc 20(9):1368–1375

Lanfranco A, Castellanos A, Desai J, Meyers W (2004) Robotic surgery: a current perspective. Ann Surg 239(1):14–21

Lim SC, Lee H, Doh E, Yun K, Park J (2014) Tactile display with tangential and normal skin displacement for robot assisted surgery. Adv Robotics 28(13):859–868

Moradi Dalvand M, Shirinzadeh B, Nahavandi S, Smith J (2014a) Effects of realistic force feedback in a robotic assisted minimally invasive surgery system. Minim Invasive Ther Allied Technol 23(3):127–135

Moradi Dalvand M, Shirinzadeh B, Shamdani AH, Smith J, Zhong Y (2014b) An actuated force feedback-enabled laparoscopic instrument for robotic-assisted surgery. Int J Med Robot 10(1):11–21

Morino M, Pellegrino L, Giaccone C, Garrone C, Rebecchi F (2006) Randomized clinical trial of robot-assisted versus laparoscopic Nissen fundoplication. Br J Surg 93(5):553–558

Muller-Stich B, Reiter M, Wente M, Bintintan V, Koninger J, Buchler M, Gutt C (2007) Robot-assisted versus conventional laparoscopic fundoplication: short-term outcome of a pilot randomized controlled trial. Surg Endosc 21(10):1800–1805

Nguan C, Girvan A, Luke P (2008) Robotic surgery versus laparoscopy; a comparison between two robotic systems and laparoscopy. J Robot Surg 1(4):263–268

Ottermo MV, Stavdahl Ø, Johansen TA (2008) Design and performance of a prototype tactile shape display for minimally invasive surgery. Haptics-E J 4(4):1–13

Reiley CE, Akinbiyi T, Burschka D, Chang DC, Okamura AM, Yuh DD (2008) Effects of visual force feedback on robot-assisted surgical task performance. J Thorac Cardiovasc Surg 135(1):196–202

Schreuder H, Verheijen R (2009) Robotic surgery. BJOG Int J Obstet Gynecol 116(2):198–213

Sung GT, Gill IS (2001) Robotic laparoscopic surgery: a comparison of the da Vinci and Zeus systems. Urology 58(6):893–898

Tholey G, Desai JP, Castellanos AE (2005) Force feedback plays a significant role in minimally invasive surgery: results and analysis. Ann Surg 241(1):102

Wottawa CR, Cohen JR, Fan RE, Bisley JW, Culjat MO, Grundfest WS, Dutson EP (2013) The role of tactile feedback in grip force during laparoscopic training tasks. Surg Endosc 27(4):1111–1118

Yoo J, Yun S, Ahn Y, Lee H, Lim S, Park J, Yun K (2014) Feedback control of pneumatic tactile actuator using capacitive displacement sensor. In: The 16th Korean MEMS conference, pp 155–156